How Shaped Light Discriminates Nearly Identical Biochromophores

Jens Petersen,[1] Roland Mitrić,[2,*] Vlasta Bonačić-Koutecký,[1,3] Jean-Pierre Wolf,[4] Jonathan Roslund,[5] and Herschel Rabitz[5]

[1]*Department of Chemistry, Humboldt-Universität zu Berlin, Brook-Taylor-Str. 2, 12489 Berlin, Germany*
[2]*Department of Physics, Freie Universität Berlin, Arnimallee 14, 14195 Berlin, Germany*
[3]*ICAST, University of Split, Meštrovićevo Šetalište bb., 21000 Split, Croatia*
[4]*GAP, University of Geneva, 20 rue de l'Ecole de Médecine, CH 1211 Geneva 4, Switzerland*
[5]*Department of Chemistry, Princeton University, Princeton, New Jersey 08544, USA*

(Received 11 May 2010; published 12 August 2010)

We present a general mechanism for successful discrimination of spectroscopically indistinguishable biochromophores by shaped light. For this purpose we use nonadiabatic dynamics in excited electronic states in the frame of the field-induced surface hopping method driven by the experimentally shaped laser fields. Our findings show that optimal laser fields drive low-frequency vibrational modes localized in the side chains of two biochromophores, thus selecting the parts of their potential energy surfaces characterized by different transition dipole moments leading to different ionization probabilities. The presented mechanism leads to selective fluorescence depletion which serves as a discrimination signal. Our findings offer a promising perspective for using optimally shaped laser pulses in bioanalytical applications by increasing the selectivity beyond the current capability.

DOI: 10.1103/PhysRevLett.105.073003 PACS numbers: 32.80.Qk, 31.15.xg, 82.37.Vb

Optimal control is based on the ability to optimize the time, phase, and frequency content of a laser field acting on a quantum system such that a chosen product state is obtained. Shaped laser fields have been successfully applied to selectively drive the dynamics in a variety of systems of interest in physics, chemistry, and biology [1–3]. Initiated by the theoretical proposal of the ''closed-loop learning'' scheme by Judson and Rabitz [4] numerous experiments have been realized, in which processes such as photochemical reactions [5–8], photoionization [9,10], high harmonic generation [11], propagation of light in nanostructures [12], etc. were controlled. The optical dynamic discrimination (ODD) of competing product channels is one of the attractive applications of the optimal control [13–16]. The principle of ODD is based on the fact that shaped laser fields can differently drive the dynamics of almost indistinguishable quantum systems. Therefore, the ODD has the potential to push the selectivity and sensitivity limit of the analytic techniques. This has been convincingly demonstrated on the example of the discrimination of the two very similar biological chromophores riboflavin (RBF) and flavin mononucleotide (FMN), which can hardly be distinguished by other spectroscopic means since they have nearly identical absorption and fluorescence spectra [16]. However, the underlying mechanism of the processes which lead to the dynamic discrimination is unknown. Moreover, a very scarce knowledge about processes responsible for selectivity of optimal control by shaped laser fields is presently available.

In this Letter, we reveal the mechanism for the optimal dynamic discrimination between riboflavin (RBF) and flavin mononucleotide (FMN) using optimally shaped laser fields. Thus, our theoretical simulation validates the general applicability of optimal control for distinguishing highly competitive product channels. The mechanism involves selection of parts of excited state potential energy surfaces (PES) by shaped laser fields from which differences in ionization between the discriminated molecules can be achieved and thus observed by differences in fluorescence depletion. This allows us not only to shed light on the control mechanism in these specific prototype systems but to predict in general how molecules with almost indistinguishable spectral features can be discriminated using shaped laser fields. The RBF and FMN molecules, which differ only in their terminal side chains [H versus $PO(OH)_2$, cf. Fig. 1], are particularly challenging systems for the optical discrimination since in both cases their main spectral features result from analogous π–π^* transitions. In order to achieve discrimination, a two-step ODD scheme

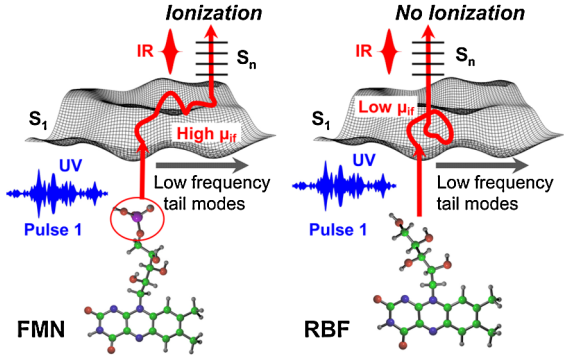

FIG. 1 (color online). Schematic illustration of the optimal dynamic discrimination by shaped laser fields on the example of shaped pulse 1 maximizing the FMN-RBF fluorescence depletion ratio.

was experimentally performed, employing a shaped UV pulse at 400 nm followed by an unshaped IR pulse at 800 nm [16]. In this way, after initial UV excitation, dynamical processes take place which are subsequently interrogated by the IR pulse, exciting the molecules to higher states and eventually evoking irreversible ionization processes. Consequently, due to the loss of population, the fluorescence of the irradiated sample is depleted. Application of the ODD yielded a UV-IR pulse pair for which the fluorescence depletion is stronger for FMN than for RBF (pulse 1), as well as a second pulse pair where the converse situation is obtained (pulse 2). In contrast, the excitation with an unshaped UV pulse leads to the same fluorescence depletion in both molecules.

We wish to show that the discriminating pulse affects differently low-frequency tail vibrational modes in the two molecules, efficiently driving one of the molecules to regions of the PES with higher transition dipole moments to higher excited states thus promoting the ionization process and enhancing the fluorescence depletion (pulse 1 for FMN). The same pulse acting on the other molecule (RBF) suppresses the ionization (depletion of fluorescence) by keeping it in regions of the PES with lower transition dipole moments as schematically presented in Fig. 1.

In order to prove this mechanism, we employ our newly developed ''field-induced surface hopping'' method (FISH) [17] which offers a unique opportunity to investigate theoretically the dynamics in complex systems and its control by laser fields accounting for all degrees of freedom and the environment. This aim can be achieved either by theoretically optimizing laser pulses in order to steer a desired process and thus to predict experimental outcomes, or the experimentally shaped laser fields can be employed in the simulation and the processes behind the control can be detected. The present Letter focuses on the second aspect.

The FISH method described previously [17] combines nuclear dynamics of an ensemble of classical trajectories with fully quantum mechanical electronic population dynamics under the influence of external time-dependent electric fields. The population transfer between the electronic states is achieved by allowing the trajectories to switch between the states. This procedure is related to Tully's surface-hopping method [18] which has been developed for the description of field-free nonadiabatic transitions in molecular systems. However, in our case the coupling between the states is also induced by the laser field. The hopping probability can be calculated from the rate of change of the excited states populations. Although the individual trajectory is allowed to jump, the total number of trajectories in a given state is a continuous function of time. The phase of the electronic wave function is preserved and our procedure gives rise to the full quantum-mechanical coherent state population. The multistate dynamics of RBF and FMN is performed in the ground (S_0) and nine excited electronic states (S_1–S_9). The electronic state populations given by $|c_i|^2$ are obtained by solving the time-dependent Schrödinger equation

$$i\hbar\dot{c}_i(t) = E_i[\mathbf{R}(t)]c_i(t) - \sum_j \{\boldsymbol{\mu}_{ij}[\mathbf{R}(t)] \cdot \mathbf{E}(\mathrm{t}) + i\hbar\dot{\mathbf{R}}(t) \cdot \mathbf{d}_{ij}[\mathbf{R}(t)]\}c_j(t) \quad (1)$$

where $\mathbf{R}(t)$ denotes the nuclear trajectory, E_i the electronic energy, $\boldsymbol{\mu}_{ij}[\mathbf{R}(t)]$ the electronic transition dipole moment, $\mathbf{E}(\mathrm{t})$ the electric laser field, and $\mathbf{d}_{ij}[\mathbf{R}(t)] = \langle\Phi_i[\mathbf{R}(t)]|\nabla_R|\Phi_j[\mathbf{R}(t)]\rangle$ labels the nonadiabatic coupling vector. Inclusion of the nonadiabatic coupling is essential since the dynamics occurs along the manifold of close-lying excited states. All quantities needed for the FISH dynamics ''on the fly'' are obtained from semiempirical electronic structure calculations using the PM3 configuration interaction method [19–21] which provides a reasonably accurate description of the electronic structure of flavins. Dissipative effects of the environment are accounted for in the frame of the Langevin dynamics, using an empirical friction constant for water [22]. Notice, that the unitary evolution described by Eq. (1) cannot lead to an irreversible loss of the electronic state population (e.g,. caused by ionization) which is responsible for fluorescence depletion. For that reason, we add in the Schrödinger equation an imaginary component to the energy of the highest excited state S_9 which lies close to the ionization limit in water [23], ensuring decay of the population. The values of the imaginary energy components for RBF and FMN are calibrated such that in analogy to the experiment identical fluorescence depletion is obtained when employing an unshaped UV-IR pulse pair. Subsequently the ionized population P_{ion} is obtained by calculating the hopping probability from the S_9 state to the ionized state. The depletion signal D is finally obtained from the P_{ion} due to both the UV and IR pulses compared to the UV pulse alone as $D = [P_{\mathrm{ion}}(\mathrm{UV}+\mathrm{IR}) - P_{\mathrm{ion}}(\mathrm{UV})]/[1 - P_{\mathrm{ion}}(\mathrm{UV})]$, where the P_{ion} are averaged over the ensemble of 30 trajectories. In order to discover the processes responsible for ODD of RBF and FMN, the experimentally optimized pulses for maximization and minimization of the depletion ratios [16] (pulse 1 and pulse 2, respectively) have been used in our FISH simulations, including approximately irreversible ionization as described above. The resulting ionized state populations together with the temporal structure of the shaped pulses are shown in Fig. 2. Both pulses consist of a shaped UV part which has a duration of about 5 ps and of a 100 fs unshaped IR component centered at $+0.5$ ps. The latter is mainly responsible for the ionization, which in the case of RBF sets in at about $+0.5$ ps. Although for FMN there is some ionization at earlier times, the main part of the ionized population is also generated at about $+0.5$ ps. The ionization yield of RBF is lower for pulse 1 than for pulse 2, whereas the reversed effect is found for FMN, proving that shaped laser fields can selectively and independently modulate the ionization yields even in almost identical molecules. The fluorescence de-

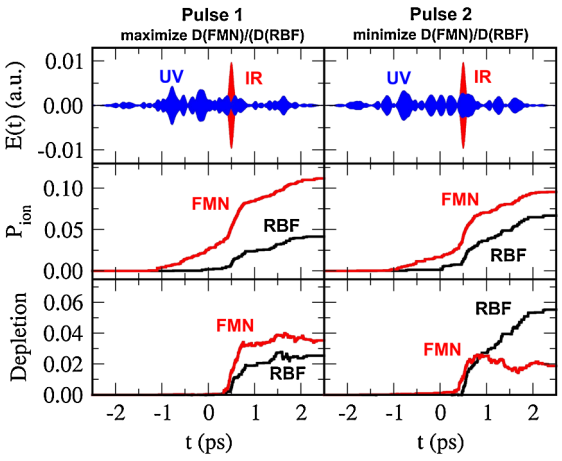

FIG. 2 (color online). Upper panel: Temporal structure of pulse 1 for maximization (left-hand side) and of pulse 2 for minimization (right-hand side) of the depletion ratio D(FMN)/D(RBF). Middle panel: Ionized populations P_{ion} of RBF (black) and FMN [grey (red)] due to pulse 1 and pulse 2. Lower panel: Fluorescence depletion D of RBF (black) and FMN [grey (red)] due to pulse 1 and pulse 2.

pletion [cf., lower part of Fig. 2] relies upon the relative decrease of the excited state population (S_1–S_9) due to both the UV and IR pulses compared to the UV pulse alone. It is initiated for both pulses and both molecules by the IR subpulse at +0.5 ps. For pulse 1, the depletion D based on the ionization mainly due to the IR pulse is systematically larger for FMN than for RBF, whereas for pulse 2 after 1 ps the depletion for RBF becomes larger than for FMN. The final fluorescence depletion ratios $D(\mathrm{FMN})/D(\mathrm{RBF})$ after the pulses have ceased are calculated to be 1.4 for pulse 1 and 0.4 for pulse 2. These values are in good agreement with the experimental ODD values of 1.3 for pulse 1 and 0.7 for pulse 2 [16]. Moreover, the calculated depletion ratio as a function of the IR pulse time delay shown in Fig. 3 supports the experimental finding that coherent dynamics occurs up to ~1 ps, thus allowing for discrimination within this time. For longer time delays the depletion ratios for both pulses come close to 1.0, thus preventing discrimination. Notice that the unshaped pulses do not discriminate [cf. Fig. 3] even at earlier times. Both theoretical findings, the ionized populations of RBF and FMN driven by pulses 1 and 2 [Fig. 2] as well as the

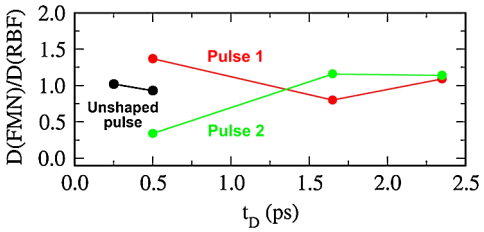

FIG. 3 (color online). Fluorescence depletion ratio as a function of the IR pulse delay for unshaped UV pulse (black), pulse 1 [dark grey (red)], and pulse 2 [light grey (green)].

calculated fluorescence depletion ratios [Fig. 3], confirm the experimental optical discrimination between FMN and RBF. Beyond that, our simulations offer a unique opportunity to gain an insight into the mechanism of dynamical processes responsible for discrimination. Since the fluorescence depletion is directly related to the ionization yield, we wish to answer how the latter can be influenced by differently shaped laser pulses. An important factor determining the ionization yield is the efficiency of populating higher excited states after initial S_0–S_1 excitation. Therefore the averaged transition dipole moments between the first and the higher excited states along the trajectories have been calculated as a measure for the efficiency of the ionization process. It can be seen from Fig. 4(a) that pulse 1 induces dynamical pathways which exhibit systematically larger transition dipole moments for FMN than for RBF, indicating the stronger ionization and accordingly stronger depletion of fluorescence in FMN. In contrast, for pulse 2 [cf. Fig. 4(b)] at times after +0.5 ps this behavior is reversed leading to higher transition dipole moments, and thus stronger fluorescence depletion for RBF. Since in our model the ionization takes place from the S_9 state mainly under the influence of the IR pulse we present in Figs. 4(c) and 4(c) the averaged transition dipole moments $\langle \mu_{n9} \rangle$ from the S_1–S_8 states to S_9 weighted by the populations of S_1–S_8. The pulse 1 invokes larger differences between these quantities in favor of FMN, while the pulse 2 leads to smaller differences between RBF and FMN. These findings are consistent with the ionization yields presented in Fig. 2. In order to establish the connection between higher transition dipole moments and the structural changes during the dynamics, the averaged time-dependent normal mode displacements along the actual trajectories have been analyzed. In general, the discriminating pulses induce conformational differences which are localized mainly in the polar side chains of both molecules. In Fig. 5 one prototype of several low-frequency normal modes of each molecule

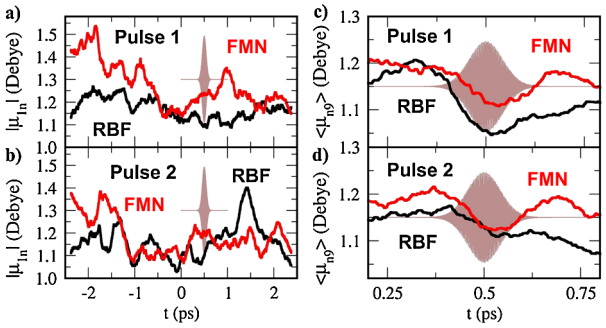

FIG. 4 (color online). (a),(b) Average transition dipole moments for $S_1 \rightarrow S_2$–S_9 transitions for the dynamics driven by pulse 1 (a) and 2 (b) for FMN [grey (red)] and RBF (black). The average is performed over the states S_2–S_9 and over the ensemble of trajectories. (c),(d) Average transition dipole moments $\langle \mu_{n9} \rangle$ for S_1–$S_8 \rightarrow S_9$ transitions weighted by the state populations as $\langle \mu_{n9} \rangle = \sum_n |c_n|^2 |\mu_{n9}|$, in the time window of the IR pulse (shaded) for pulse 1 (c) and 2 (d).

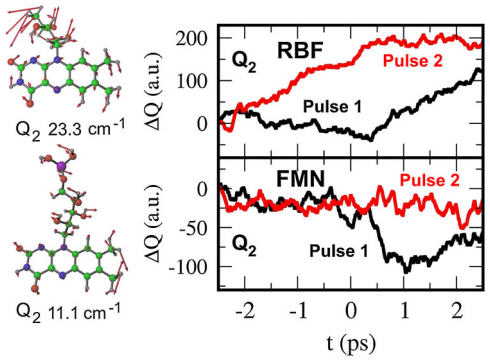

FIG. 5 (color online). Selected averaged ground state normal mode displacements for RBF (upper panel) and FMN (lower panel) induced by pulse 1 (black) and pulse 2 [grey (red)].

exhibiting large displacements induced by pulses 1 and 2 is shown. The excitation of these low-frequency modes differs considerably depending on which pulse is acting on the system. The pulse 1 invokes smaller deviations for the normal coordinate Q_2 in RBF and larger deviations after 0 ps for Q_2 in FMN compared to pulse 2. Thus, the excitation of low-frequency normal modes leads to population of conformations which have systematically higher or lower transition dipole moments to higher excited states leading to ionization, depending on which of the two discriminating pulses is acting. Since RBF and FMN only differ in the side chain, differences in the dynamical behavior should occur here due to the interplay between the effect of the heavy phosphorus atom in FMN and the differences of the vibrational density of states in both molecules.

In summary, the following picture of the discrimination process emerges [cf. Fig. 1]: UV excitation of the molecule induces dynamical processes in excited states which mainly affect low-frequency tail vibrational modes. The discriminating pulse drives one of the molecules to regions of the PES where the transition dipole moments to higher excited states are high and thus the ionization and the fluorescence depletion are enhanced (pulse 1 for FMN). The same pulse acting on the other molecule (RBF) suppresses the ionization (depletion of fluorescence) by keeping it in regions of the PES with lower transition dipole moments. Thus, in general, the shaped pulses can take advantage of minute differences in vibrational dynamics and exploit them to manipulate observables such as transition dipoles, allowing for the selective molecular discrimination. This mechanism represents a general feature that can be exploited for the discrimination between similar molecules and offers a promising tool for using optimally shaped laser pulses in bioanalytical applications, thus increasing the selectivity beyond the current capability.

This work has been supported by the Deutsche Forschungsgemeinschaft (DFG), SFB 450. Financial support in the frame of the DFG Emmy Noether program (MI-1236) (R. M.), of the Fonds der Chemischen Industrie (J. P.) and of the Swiss SNF within the "MUST" NCCR network (J.-P. W.) is also acknowledged.

*mitric@zedat.fu-berlin.de

[1] S. A. Rice and M. Zhao, *Optical Control of Molecular Dynamics* (John Wiley & Sons, New York, 2000).
[2] P. W. Brumer and M. Shapiro, *Principles of the Quantum Control of Molecular Processes* (Wiley-VCH, Berlin, 2003).
[3] *Analysis and Control of Ultrafast Photoinduced Reactions*, edited by L. Wöste and O. Kühn, Springer Series in Chemical Physics Vol. 87 (Springer, New York, 2007).
[4] R. S. Judson and H. Rabitz, Phys. Rev. Lett. **68**, 1500 (1992).
[5] A. Assion, T. Baumert, M. Bergt, T. Brixner, B. Kiefer, V. Seyfried, M. Strehle, and G. Gerber, Science **282**, 919 (1998).
[6] C. Daniel, J. Full, L. Gonzalez, C. Lupulescu, J. Manz, A. Merli, S. Vajda, and L. Wöste, Science **299**, 536 (2003).
[7] T. Brixner and G. Gerber, Chem. Phys. Chem. **4**, 418 (2003).
[8] G. Vogt, G. Krampert, P. Niklaus, P. Nuernberger, and G. Gerber, Phys. Rev. Lett. **94**, 068305 (2005).
[9] B. Schäfer-Bung, R. Mitrić, V. Bonačić-Koutecký, A. Bartelt, C. Lupulescu, A. Lindinger, S. Vajda, S. M. Weber, and L. Wöste, J. Phys. Chem. A **108**, 4175 (2004).
[10] V. Bonačić-Koutecký and R. Mitrić, Chem. Rev. **105**, 11 (2005).
[11] C. Winterfeld, C. Spielmann, and G. Gerber, Rev. Mod. Phys. **80**, 117 (2008).
[12] M. Aeschlimann, M. Bauer, D. Bayer, T. Brixner, F. J. de Abajo, W. Pfeiffer, M. Rohmer, C. Spindler, and F. Steeb, Nature (London) **446**, 301 (2007).
[13] T. Brixner, N. H. Damrauer, P. Niklaus, and G. Gerber, Nature (London) **414**, 57 (2001).
[14] B. Li, G. Turinici, V. Ramakrishna, and H. Rabitz, J. Phys. Chem. B **106**, 8125 (2002).
[15] B. Li, H. Rabitz, and J.-P. Wolf, J. Chem. Phys. **122**, 154103 (2005).
[16] M. Roth, L. Guyon, J. Roslund, V. Boutou, F. Courvoisier, J.-P. Wolf, and H. Rabitz, Phys. Rev. Lett. **102**, 253001 (2009).
[17] R. Mitrić, J. Petersen, and V. Bonačić-Koutecký, Phys. Rev. A **79**, 053416 (2009).
[18] J. C. Tully, J. Chem. Phys. **93**, 1061 (1990).
[19] J. J. P. Stewart, J. Comput. Chem. **10**, 209 (1989).
[20] A. Koslowski, M. E. Beck, and W. Thiel, J. Comput. Chem. **24**, 714 (2003).
[21] S. Patchkovskii, A. Koslowski, and W. Thiel, Theor. Chem. Acc. **114**, 84 (2005).
[22] W. F. van Gunsteren and H. J. C. Berendsen, Mol. Phys. **45**, 637 (1982).
[23] N. Getoff, S. Solar, and D. B. McCormick, Science **201**, 616 (1978).